Pergamon

Bioorganic & Medicinal Chemistry, Vol. 5, No. 6, pp 1063–1069, 1997

PII: S0968-0896(97)00042-4
0968-0896/97 $17.00 + 0.00

Construction of Hairpin Ribozymes with a Three-Way Junction

Yasuo Komatsu, Miho Shirai, Shigeko Yamashita and Eiko Ohtsuka*
Faculty of Pharmaceutical Sciences, Hokkaido University, Sapporo 060, Japan

Abstract—Hairpin ribozymes with high cleavage activities were designed. An extra sequence was introduced at the 3′-end of the hairpin ribozyme to increase the binding to the substrate RNA, as compared to the wild-type hairpin ribozyme. A three-way junction (TWJ) was formed between the newly designed ribozyme and the substrate RNA. The complex with a solid TWJ showed less RNA cleavage activity than the wild-type hairpin ribozyme. However, the ribozyme with a TWJ with five unpaired bases or propandiol phosphate linkers had higher cleavage activity than the parent ribozyme without the TWJ. When a *cis*-cleavage system, in which the 5′-end of the substrate RNA was conjugated to the 3′-end of the ribozyme, was employed, the complex with the TWJ containing unpaired bases was also cleaved faster than the complex with the solid TWJ. This suggested that these differences in the cleavage activities were derived from the conformation, and this was proven by nondenaturing gel electrophoresis. The TWJ hairpin ribozyme containing unpaired bases is able to bind strongly with substrate RNAs and to cleave them efficiently. Since the three-way ribozyme presented here is more active than the wild-type ribozyme, this type of ribozyme can serve as a more efficient tool to control RNA activities in vitro and in vivo. © 1997 Elsevier Science Ltd.

Introduction

The hairpin ribozyme was discovered within 359 bases of the negative strand of the satellite RNA of tobacco ring spot virus.[1–4] The satellite RNA is replicated to generate multimeric complementary positive strands by RNA polymerase in the host plant. Strands of both polarities are autoprocessed to monomeric forms during replication. The catalytic centers of the negative and positive strands have been identified: that of the negative strand is called a hairpin ribozyme, and that of the positive strand is a hammerhead ribozyme.[5] The hairpin ribozyme consists of 50 bases and can cleave RNA catalytically, depending on the sequence (Fig. 1a).[3,6,7] The cleavage reaction proceeds by an in-line mechanism,[8] in the presence of divalent metal ions, to generate a 5′-hydroxyl group and a 2′,3′-cyclic phosphate.[1] This ribozyme has two helix-loop domains, in which there are two helices and an internal loop (loop A in domain I and loop B in domain II in Fig. 1a). Required bases for the cleavage activity have been investigated vigorously by random selection[9–11] and point mutation experiments,[12–14] and most of the essential bases have been shown to exist in the two internal loop regions. The secondary structures of the two domains were studied by chemical modification,[15] incorporation of nucleotide analogs,[16] and photo-cross-linking,[17–19] and it was suggested that there are noncanonical base pairs in both internal loops. Recently, the three-dimensional structure of domain I alone, which was not conjugated with domain II, has been determined by nuclear magnetic resonance (NMR) spectroscopy.[20] From these data, a sheared G.A base pair was shown to exist, and a uracil next to the cleavage site on the 3′-side was splayed apart in loop A. It was suggested that this characteristic structure was recognized by loop B in domain II.

The overall structure of the hairpin ribozyme is still unknown. We have investigated the structure–function relationship of the hairpin ribozyme. First we indicated that the hairpin ribozyme can be divided into two fragments at its hairpin loop J3, shown in Figure 1b, and maintain the cleavage activity.[12] We next introduced various numbers of propandiol phosphate linkers in J1 of the parent ribozyme (Fig. 1b).[21] Since the cleavage activities depended on the linker lengths in the experiment, a bent conformation for the two domains was proposed. The same result was obtained by Feldstein and Bruening.[22] It was also proven that J2 could be separated by connecting J1.[23] Furthermore, we have constructed a reversely joined ribozyme, in which both J1 and J2 were separated, but J4 was linked covalently using nucleotide linkers.[23] These reversely joined ribozymes had cleavage activities nearly equal to that of the wild-type. Burke et al. showed that the cleavage reaction was also detected in the completely separated two domains, in the presence of a high magnesium ion concentration.[24] Recently, we also showed that the cleavage reaction occurred in the completely divided two domains, with a low magnesium ion concentration, if a complementary anchor region was paired by hydrogen bonds.[25] These results confirm that the active conformation of the hairpin ribozyme is a bent form.

Recently, ribozymes have been applied to the cleavage of mRNA in vivo to suppress the expression of genes for cancer or human immunodeficiency virus.[26–30] In most of these approaches, the ribozyme genes are transfected into the cells by a vector. For these approaches, the construction of a new ribozyme with high cleavage activity is important. We intend to extend the use of ribozymes to other systems of biological interest. Nitric oxide (NO) is synthesized from L-arginine by nitric

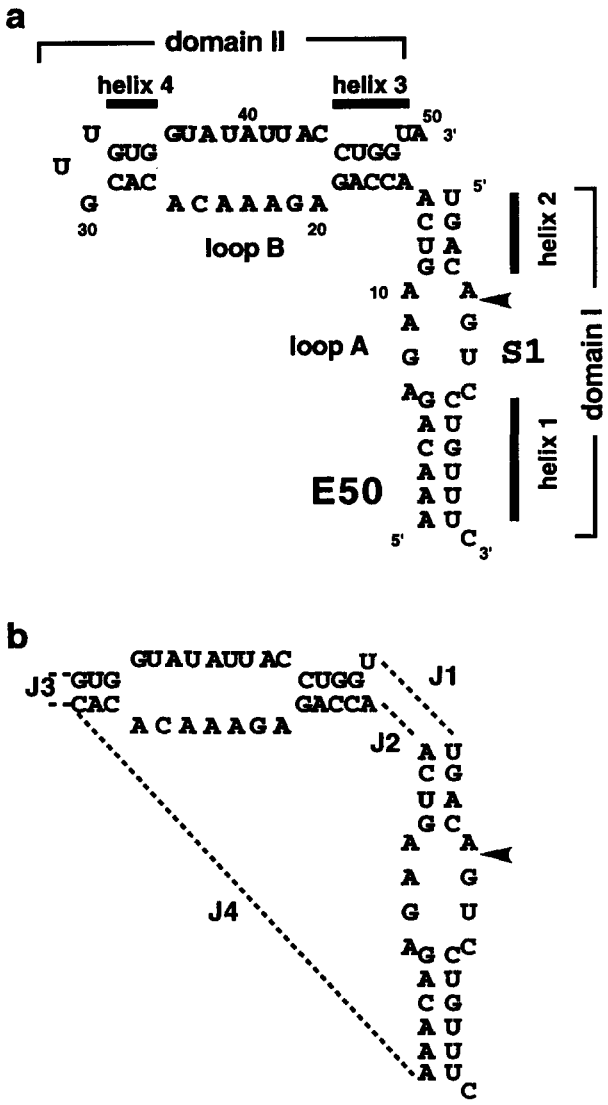

Figure 1. Secondary structures of hairpin ribozymes. (a) A wild-type hairpin ribozyme (E50) and a substrate (S1). Domain I involves helix 1, helix 2, and an internal loop A; and domain II, helix 3, helix 4, loop B, and a hairpin loop (GUU). (b) Modified hairpin ribozymes constructed for studies of structure–function relationships. The covalent bonds of J1 and J4 do not exist in the natural hairpin ribozyme, while bond J2 conjugates the two domains in the wild-type ribozyme. J2 can be separated when J1 is connected. When domain I and domain II were connected by J4, the two domains were aligned in a reversely joined ribozyme. Cleavage occurred with dependence on the linker lengths at J1 and J4.

oxide synthases and has many biological functions.[31] It has been shown that NO derived from the induced nitric oxide synthase (iNOS) in the brain causes neuronal death.[32] We present here a new type of hairpin ribozyme that specifically cleaves the iNOS mRNA. This new type of ribozyme has an extra sequence at the 3′-side of the wild-type ribozyme to allow it to hybridize with the 5′-side sequence of the substrate. This ribozyme can form a rigid three-way structure at the ribozyme–substrate junction. When unpaired bases were inserted in the three-way junction (TWJ) of the ribozyme, a higher cleavage activity was obtained as compared to the wild-type hairpin ribozyme. This is the first report of the introduction of such a sequence into a ribozyme to increase the catalytic activity. The TWJs with unpaired bases did not disturb the formation of the active bent structure, but assisted in the the formation of the active conformation. The ribozymes described here are of interest not only for their activities of ribozyme but also for the tertiary structures of the RNA.

Results and discussion

Construction and reaction of three-way ribozymes targeting mRNA for iNOS

As the substrate, a 19-base RNA with the sequence from codons 34–40 of iNOS[33] was synthesized (iNOS19, Fig. 2). Five ribozymes were designed to cleave iNOS19, as shown in Figure 2. Complex 1 involves both iNOS19 and a wild-type hairpin ribozyme (R32+R21), which has only 10 base pairs formed in both helix 1 and helix 2. Ribozymes possessing a new binding manner were constructed to increase the cleavage activity (TW, TW-A5 and TW-Pn, Fig. 2). It is expected that in these ribozymes helix 5 would be newly formed and consequently, TWJs would be created. The two stranded ribozyme TW(R32+R25) binds to iNOS19 to form the complex TW/iNOS19, which has a solid TWJ. On the other hand, the ribozyme TW-A5 (R32+R25A5) has five unpaired adenine bases at the linker region (Fig. 2), and TWJ containing unpaired bases are formed in the complex TW-A5/iNOS19. To investigate the influence of the linker sequence on the cleavage activity, two ribozymes with propandiol phosphate linkers (PPL)[21] at TWJs, were constructed (TW-P2 and TW-P5). These ribozymes also can form TWJs by binding with iNOS19. Although the 5′-side sequences of these ribozymes were the same (R32), the 3′-side sequences of them were different. Since the additional helix 5 is formed in these complexes, the turnover abilities of these ribozymes were expected to be low. Thus, the number of base pairs in helix 1 for all of ribozymes used here was decreased from six to five base pairs to facilitate the turnover, although hairpin ribozymes are generally designed to contain six base pairs in helix 1.[6]

Cleavage reactions with these ribozymes were carried out under multiple turnover conditions. iNOS19 was cleaved at the expected, unique, site by all of the ribozymes. The kinetic parameters were measured and are shown in Table 1. The K_m values were almost the same for the five ribozymes; however, the k_{cat} value of the TW-A5/iNOS19 complex was higher than those of the other complexes, and the k_{cat}/K_m value of TW-A5/iNOS19 was about two- and fourfold higher than those of complex 1 and TW/iNOS19, respectively. The cleavage activity of TW was lower than that of TW-A5, which contains unpaired adenine tracts at the TWJ. These results suggest that adenine bases at the TWJ of TW-A5 might play important roles for increased activity. Ribozyme TW-P5, with five PPLs, showed almost the same activity as TW-A5. This result indicates

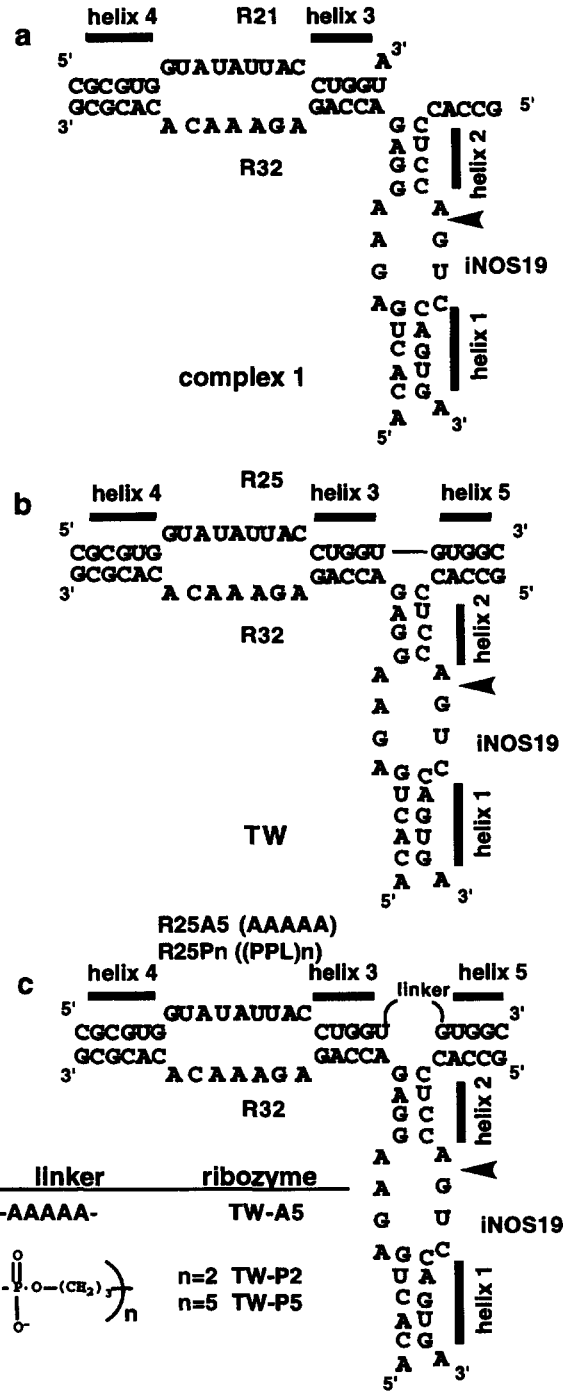

Figure 2. Sequences of three hairpin ribozymes and a 19-mer substrate (iNOS19). (a) Complex 1 contains a wild-type hairpin ribozyme (R32-R21). (b) TW contains a two stranded ribozyme (R32-R25) and forms a three-way junction with the substrate. (c) TW-A5 and TW-P*n* contain two stranded ribozymes (R32-R25A5 and R32-R25P*n*; n = 2 or 5) that form a three-way junction with the substrate. The letter R and the following numbers indicate ribozyme strand and number of bases. Arrows indicate cleavage sites.

that the high cleavage activity of TW-A5 was not derived from the sequence of the linker.

The K_m values for these complexes were relatively high, as compared with that reported previously for the hairpin ribozyme.[3] This may be a consequence of shortening helix 1 to prevent the decrease of the turnover ability of the three-way hairpin ribozyme. In complex 1, the ribozyme bound with the substrate RNA by only nine base pairs in helix 1 and helix 2, and since complex 1 did not contain the additional helix 5, the instability of helix 1 may be reflected in the high K_m value. The K_m values of other ribozymes (TW-A5 and TW-P5) were also not improved by the addition of helix 5. However, helix 5 seemed to influence the k_{cat} values rather than the affinity to the substrate (Table 1). Perhaps the formation of the active conformation of the ribozymes might be more effectively assisted by helix 5 and the linker region. The K_m values of TW-P*n* were somewhat smaller than those of TW and TW-A5. This may be because TW and TW-A5 folded like a duplex before substrate binding, and the affinity to the substrate might be lower than that of TW-P*n*.

Table 1. Kinetic parameters of the three complexes

Ribozyme	K_m (μM)	k_{cat} (min^{-1})	k_{cat}/K_m (rel)
R32–R21	0.14	0.40	1.0
TW (R32–R25)	0.11	0.20	0.65
TW-A5 (R32–R25A5)	0.11	0.72	2.2
TW-P2 (R32–R25P2)	0.023	0.044	0.65
TW-P5 (R32–R25P5)	0.083	0.60	2.5

k_{cat}/K_m are listed as relative values to R32-R21, which is the ribozyme portion of complex 1.

TW-P2, which contains two PPLs, did not cleave as fast as TW-P5, but did cleave the substrate. The low activity of TW-P2 suggests that two PPLs cannot give enough flexibility in the branched point. TWJs of DNA have been studied extensively by native gel analysis[34,35] and NMR.[36–38] The three helices are extended with the same angles as in the DNA TWJ, in the absence of unpaired bases at the hinge. On the other hand, when extra bases are inserted in the branched point of the DNA TWJ, the three helices are not positioned with equivalent angles. One angle in the junction becomes smaller than the other two. These features of TWJs containing unpaired bases are caused by metal ions. It also has been shown that bases at the branched point of the junction play an important role in the relative locations of the three helices.[35] These data suggest that TWJ can induce unusual structures by the insertion of unpaired bases. These characteristics have not been reported for the TWJ of RNA; however, hammerhead ribozymes possess a type of three-way structure, and the overall structures have been investigated in detail by X-ray,[39,40] fluorescence energy transfer,[41] and native polyacrylamide gel analysis.[42] According to these data, the three-helices of the hammerhead ribozyme are aligned similarly to the DNA TWJ with unpaired bases, and the structure of the three stems also depends on Mg^{2+} ion concentration.

There seem to be many differences in the conformations of the junction of TW/iNOS19 and TW-A5/iNOS19. The interaction between domain I and domain II might be poor in the complex TW/iNOS19, because the three helices at the junction are equally extended.

On the other hand, a domain–domain interaction might occur in TW-A5/iNOS19 or TW-P5/iNOS19, since the structural stress originating in the TWJ of these complexes might be released by the unpaired adenine or the PPL tract, and the flexibilities of the three helices might increase the domain–domain interaction. The difference in the activities between TW-P2 and TW-P5 suggests that the flexibility of TWJ is important for the cleavage.

Gel mobility shift assay of complexes with TWJs

To investigate the differences in the conformations of complex 1, TW/iNOS19, and TW-A5/iNOS19, a gel mobility shift analysis was carried out. Since the complex formation was performed in the presence of magnesium ions, an uncleavable substrate analogue, DNOS19 (5′GCCACCUCCdAGUCCAGUGA3′), containing deoxyadenosine instead of adenine at the 5′-side of the cleavage site, was used for the gel shift analysis. Each complex contained DNOS19. Complex formation was observed in all cases (R32-R21/DNOS19, TW-A5/DNOS19, TW-A5/DNOS19, Fig. 3). Complex R32-R21/DNOS19 moved fastest in the gel among the complexes, since its molecular weight was lowest (lane 1 in Fig. 3). Interestingly, TW/DNOS19 migrated slower than TW-A5/DNOS19, although the molecular weight of TW/DNOS19 was smaller than that of TW-A5/DNOS19 (lanes 2 and 3 in Fig. 3). The reason for this difference in the migrations is not clear; however, this result suggests that the conformations of TW/DNOS19 and TW-A5/DNOS19 are different. TW-A5/DNOS19 may be more compact than TW/DNOS19, because domain I might be close to domain II, due to the flexibility of the branched point of the TWJ of TW-A5/DNOS19.

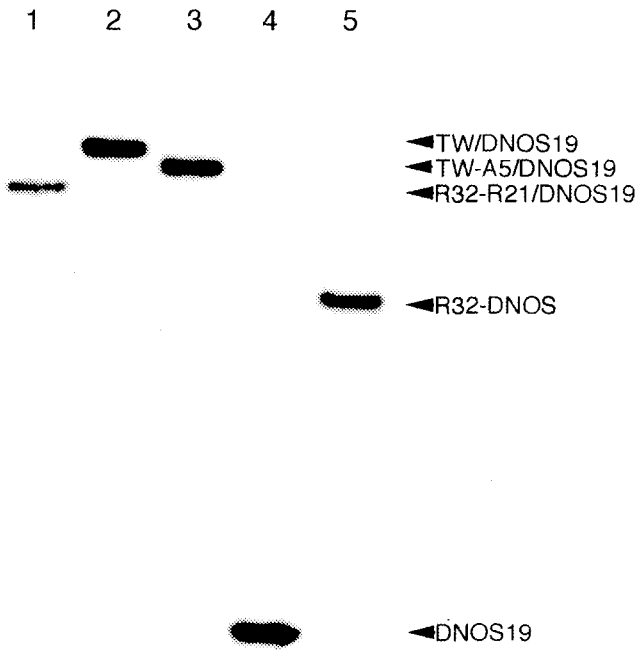

Figure 3. Autoradiogram of a 10% native polyacrylamide gel (acrylamide:bisacrylamide, 29:1) after electrophoresis of R32-R21 and the three-way ribozymes. The 5′-labeled DNOS19 was mixed with ribozymes (R32-R21, TW, or TW-A5). Lane 1, R32-R21/DNOS19; lane 2, TW/DNOS19; lane 3, TW-A5/DNOS19; lane 4, DNOS19; lane 5, R32-DNOS19.

Cis-cleavage systems for three-way ribozymes

Since helix 5 consists of five base pairs, it was thought that helix 5 was not stable and was not formed exactly during the cleavage reactions. To confirm the formation of helix 5 in TW/iNOS19 and TW-A5/iNOS19 (Fig. 2), RNAs for *cis*-cleavage were prepared. As substrates in these complexes, the 3′-end of R25 of TW or the R25A5 of TW-A5 was conjugated with the 5′-end of iNOS19 by a stable hairpin loop (GAAA),[43] and they were referred to as RNOS and RNOSA5 (Fig. 4). The only difference between them is the presence of five adenine bases in the linker in RNOSA5. RNOS and RNOSA5 can form TWJs with R32. Cleavage reactions were carried out

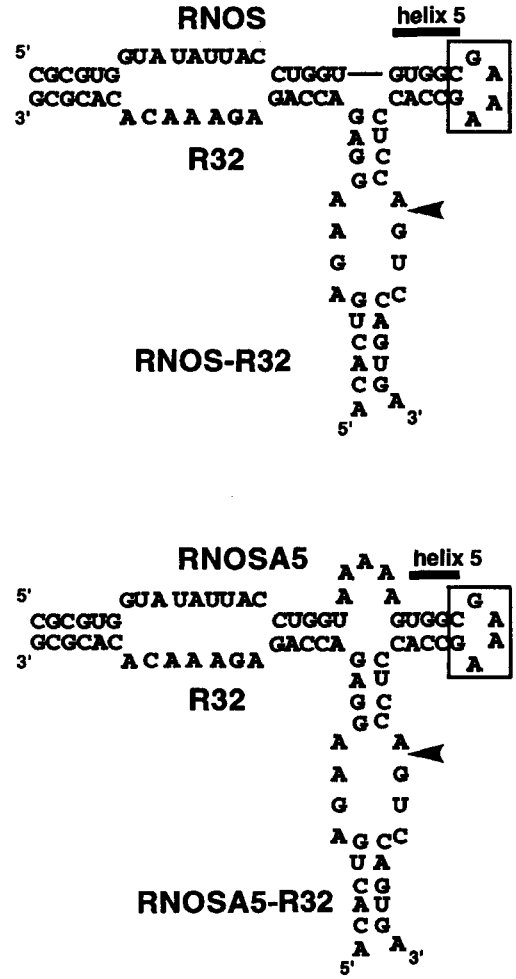

Figure 4. Complexes used for *cis*-cleavage systems. RNOS and RNOSA5 have continuous sequences from the 3′-side sequence of the ribozymes for iNOS19. Each is joined by a stable hairpin loop (GAAA). Cleavage sites and stable loops are indicated by arrows and boxes.

under single turnover conditions, because the products from these complexes could incorporate another RNOS (RNOSA5) molecule as a substrate under conditions of excess substrate. RNOSA5 was found to be cleaved about four times faster than RNOS in the presence of R32 (Table 2). This result is consistent with the cleavage of iNOS19 described above. Since the TWJs seemed to be formed as expected in the R32-RNOS and R32-RNOSA5 complexes in the presence of the stable hairpin loop, it was confirmed that the differences in the cleavage activities were derived from the structure of the TWJ. This result is consistent with that of the gel mobility shift assay. Unpaired adenine bases at the TWJs must play an important role in the high cleavage activity of TW-A5.

Conclusion

Hairpin ribozymes involving TWJs were constructed. These ribozymes were designed to cleave a part of the sequence of the iNOS mRNA from the human glioblastoma cell line A-172. In these ribozymes, a new stem (helix 5) was introduced and the number of base pairs in helix 1 was decreased to obtain high catalytic efficiency. The ribozyme containing a solid TWJ (TW, Fig. 2) showed lower cleavage activities than the wild-type ribozyme; however, the ribozyme with a flexible TWJ consisting of extra adenine bases (TW-A5, Fig. 1), exhibited higher cleavage activity than the parent ribozyme. Linker sequences inserted at the TWJ did not influence the high cleavage activity, because a ribozyme with propandiol phosphate linkers at the TWJ (TW-P5) also indicated high cleavage activity, similar to that of TW-A5. The kinetic data suggest that the newly formed helix 5 facilitated the formation of the active conformation rather than the affinity to the substrate RNA.

Furthermore, a *cis*-cleavage ribozyme containing a TWJ with extra bases (RNOSA5, Fig. 4) also showed more efficient cleavage than the ribozyme with a solid TWJ (RNOS, Fig. 4). From native gel analysis, it was suggested that these differences in the cleavage activities were derived from their conformations (Fig. 3). A schematic drawing of the structures of TW/iNOS19 and TW-A5/iNOS19 is shown in Figure 5. Since the domain–domain interaction may be restrained by the rigid TWJ of TW/iNOS19, two domains seem to have difficulty approaching each other in the complex. However, domain I may be able to approach domain II, due to the flexibility of the TWJ in TW-A5/iNOS19. The conformations shown in Figure 5 might be favored ones of each complex. TW-A5/iNOS19 may be stabilized by the introduction of helix 5. An mRNA with a highly ordered structure is difficult to cleave with ribozymes, because binding of the ribozyme to such substrate RNAs is prevented. However, the ribozymes designed here, such as the TW-A5, are able to bind an RNA with a highly ordered structure more efficiently, due to the additional base pairs formed between the ribozyme and the target RNA. Thus, the present ribozyme with the new binding stem for the target RNA, will become a useful tool to control RNA activities.

Table 2. Single turnover rate constants (k_{cl}) of *cis*-cleavage ribozymes

	R32-RNOS	R32-RNOSA5
k_{cl} (min^{-1})	0.18	0.71

Experimental

Preparation of RNA

All RNAs were chemically synthesized by the phosphoroamidite method using 2′-*O*-(*tert*-buthyldimethylsilyl)-5′-*O*-(dimethoxytrityl)-3′-*O*-[(*N,N*-diisopropylamino)-(β-cyanoethoxy)phosphino]-nucleotides, which were purchased from GLEN research. The synthesis was carried out with an Applied Biosystems DNA/RNA synthesizer (model 394A). Deprotection of synthesized RNAs was performed as reported previously,[23] and these RNAs were purified by reverse-phase and anion-exchange HPLC using μ-Bondasphere (C-18), 3.9 mm id × 150 mm (Waters) and TSK gel DEAE-2SW, 4.6 mm id × 250 mm (Tosoh) columns, respectively. 1,3-Propandiol linkers (PPLs) were inserted in RNAs using 1-*O*-(4,4′-dimethoxytrithyl)-3-*O*-[(*N,N*-diisopropylamino)-(β-cyanoethoxy)phosphino]-1,3-propanediol, which was synthesized as described previously.[21,44]

The 5′-ends of iNOS19 and DNOS19 were labeled with [γ-^{32}p]ATP and T4 polynucleotide kinase A-19 (Takara Shuzo Co. Ltd.). The 3′-ends of RNOS and RNOSA5 were labeled with [5′-^{32}p]pCp and RNA ligase as described previously.[45]

Cleavage reactions of iNOS19

Ribozyme solutions combining R32 with R21, R25, or R25A5 were prepared, and dissolved in the cleavage buffer (40 mM Tris–HCl (pH 7.5), 12 mM $MgCl_2$, 2 mM spermidine–3HCl). Ribozyme solutions (32 nM, 50 μL) were heated at 90 °C for 2 min, rapidly cooled on ice, and incubated on ice for 10 min. To initiate the cleavage reaction, an equal volume of the ribozyme was added to the 5′-end labeled iNOS19 (43–400 nM, 8 μL), which was dissolved in the cleavage buffer and denatured by

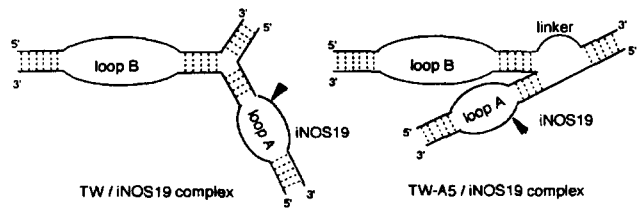

Figure 5. Possible conformations of the TW/iNOS19 and TW-A5/iNOS19 complexes. Solid lines and dotted lines indicate the continuous RNA strands and base pairs, respectively. Cleavage sites are shown by arrows.

preheating at 90 °C for 2 min, followed by rapid cooling in ice bath. The final concentrations of the ribozyme was 16 nM in the reaction solution. The cleavage reactions were performed at 37 °C. Aliquots were taken at time intervals and the reactions were stopped by transferring the aliquots into loading solution (50 mM Na_2EDTA, 10 M urea and 0.1% (w/v) bromophenol blue). The aliquots were fractionated by electrophoresis on a 20% polyacrylamide gel containing 8 M urea, and the percentages of the cleaved products were estimated by measuring the radioactivities using a Bioimaging analyzer (FUJIX BAS 2000). The kinetic constants, k_{cat} and K_m, were determined from a Hanes–Woolf plot, obtained from initial velocities.

Cleavage reactions of RNOSA5 or RNOS

RNOS and RNOSA5 were each dissolved in cleavage buffer to a concentration 40 nM, respectively, and R32 (4 μM) dissolved in cleavage buffer was prepared. RNOS or RNOSA5 (40 nM; 12 μL) and R32 (4 μM; 20 μL) were separately heated at 90 °C for 2 min, then transferred to an ice bath. An equal volume of R32 was added to the RNOS or RNOSA5 solution, and the mixture was incubated at 37 °C. Aliquots were taken at time intervals, and were added to loading solution (50 mM Na_2EDTA, 10 M urea, and 0.1% (w/v) bromophenol blue) to stop the reactions. Percentages of cleavage were calculated by the same method as for the reaction of iNOS19 described above.

Nondenaturing gel electrophoresis

Ribozyme strands (200 nM; 50 μL) and 5′-end labeled substrates (DNOS19; 40 nM, 5 μL) were dissolved in cleavage buffer (40 mM Tris–HCl (pH 7.5), 12 mM $MgCl_2$, 2 mM spermidine-3HCl) containing 3% glycerol, 0.1% (w/v) xylene cyanol, and 0.1% (w/v) bromophenol blue. The aliquots containing ribozyme were heated at 90 °C for 2 min, and then transferred into an ice bath. An equal volume of ribozyme solution was mixed with a substrate solution (DNOS19), which was denatured previously by heating at 90 °C for 2 min and then cooling in an ice bath. After the combined solution was incubated at 37 °C for 1 h, the complexes were separated by nondenaturing 10% polyacrylamide gel (acrylamide:bisacrylamide, 29:1) electrophoresis, which was carried out at 4 °C, using 40 mM Tris–acetate (pH 7.5) and 12 mM magnesium acetate buffer.

Acknowledgements

This work was supported by a Special Coordination Funds for Promoting Science and Technology of the Science and Technology Agency of the Japanese Government, and a Grant-in-Aid from the Ministry of Education, Science and Culture of Japan. The authors thank Professor Nomura and Dr T. Uehara for the iNOS sequences and Dr M. Koizumi for helpful discussion.

References

1. Buzayan, J. M.; Gerlach, W. L.; Bruening, G. *Nature (London)* **1986**, *323*, 349.

2. Haseloff, J.; Gerlach, W. L. *Gene* **1989**, *82*, 43.

3. Hampel, A.; Triz, R. *Biochemistry* **1989**, *28*, 4929.

4. Feldstein, P. A.; Buzayan, J. M.; Bruening, G. *Gene* **1989**, *82*, 53.

5. Symons, R. H. *Annu. Rev. Biochem.* **1992**, *61*, 641.

6. Hampel, A. T., R.; Hicks, M.; Cruz, P. *Nucleic Acids Res.* **1990**, *18* ,299.

7. Feldstein, P. A.; Buzayan, J. M.; Van Tol, H.; deBear, J.; Gough, G. R.; Gilham, P. T.; Bruening, G. *Proc. Natl. Acad. Sci. U.S.A.* **1990**, *87*, 2623.

8. van Tol, H.; Buzayan, J. M. F. P. A.; Eckstein, F.; Bruening, G. *Nucleic Acids Res.* **1990**, 1971.

9. Berzal-Herranz, A.; Joseph, S.; Burke, J. M. *Genes Dev.* **1992**, *6*, 129.

10. Berzal-Herranz, A.; Joseph, S.; Chowrira, B. M.; Butcher, S. E.; Burke, J. M. *EMBO J.* **1993**, *12*, 2567.

11. Joseph, S.; Berzal-Herranz, A.; Chowrira, B. M.; Butcher, S.; Burke, J. M. *Genes Dev.* **1993**, *7*, 130.

12. Sekiguchi, A.; Komatsu, Y. K., M.; Ohtsuka, E. *Nucleic Acids Res.* **1991**, *19*, 6833.

13. Chowrira, B. M.; Berzal-Herranz, A.; Burke, J. M. *Nature (London)* **1991**, *354*, 320.

14. Anderson, P.; Monforte, J.; Tritz, R.; Nesbitt, S.; Hearst, J.; Hampel, A. *Nucleic Acids Res.* **1994**, *22*, 1096.

15. Butcher, S. E.; Burke, J. M. *J. Mol. Biol.* **1994**, *244*, 52.

16. Grasby, J. A.; Gait, M. J. *Biochemistry* **1994**, *76*, 1223.

17. dos Santos, D. V.; Fourrey, J. L.; Favre, A. *Biochem. Biophys. Res. Commun.* **1993**, *190*, 377.

18. dos Santos, D. V.; Vianna, A. L.; Fourrey, J. L.; Favre, A. *Nucleic Acids Res.* **1993**, *21*, 201.

19. Butcher, S. E.; Burke, J. M. *Biochemistry* **1994**, *33*, 992.

20. Cai, Z. P.; Tinoco, I. *Biochemistry* **1996**, *35*, 6026.

21. Komatsu, Y.; Koizumi, M.; Nakamura, H.; Ohtsuka, E. *J. Am. Chem. Soc.* **1994**, *116*, 3692.

22. Feldstein, P. A.; Bruening, G. *Nucleic Acids Res.* **1993**, *21*, 1991.

23. Komatsu, Y.; Kanzaki, I.; Koizumi, M.; Ohtsuka, E. *J. Mol. Biol.* **1995**, *252*, 296.

24. Butcher, S. E.; Heckman, J. E.; Burke, J. M. *J. Biol. Chem.* **1995**, *270*, 29648.

25. Komatsu, Y; Kanzaki, I; Ohtsuka, E. *Biochemistry* **1996**, *35*, 9815.

26. Ojwang, J. O.; Hampel, A.; Looney, D. J.; Wong-Staal, F. *Proc. Natl. Acad. Sci. U.S.A.* **1992**, *89*, 10802.

27. Yu, M.; Ojwang, J.; Yamada, O.; Hampel, A.; Rapapport, J.; Looney, D.; Wong-Staal, F. *Proc. Natl. Acad. Sci. U.S.A.* **1993**, *90*, 6340.

28. Yamada, O.; Yu, M.; Yee, J. K.; Kraus, G.; Looney, D.; Wongstaal, F. *Gene Therapy* **1994**, *1*, 38.

29. Zhou, C.; Bahner, I. C.; Larson, G. P.; Zaia, J. A.; Rossi, J. J.; Kohn, D. B. *Gene* **1994**, *149*, 33.

30. Heidenreich, O.; Kang, S. H.; Brown, D. A.; Xu, X.; Swiderski, P.; Rossi, J. J.; Eckstein, F.; Nerenberg, M. *Nucleic Acids Res* **1995**, *23*, 2223.

31. Moncada, S.; Palmar, R. M.; Higgs, E. A. *Pharmacol. Rev.* **1991**, *43*, 109.

32. Nomura, Y.; Kitamura, Y. *Neurosci. Res.* **1993**, *18*, 103.

33. Hokari, A.; Zeniya, M.; Esumi, H. *J. Biochem.* **1994**, *116*, 575.

34. Welch, J. B.; Duckett, D. R.; Lilley, D. M. J. *Nucleic Acids Res.* **1993**, *19*, 4548.

35. Welch, J. B.; Walter, F.; Lilley, D. M. J. *J. Mol. Biol.* **1995**, *251*, 507.

36. Rosen, M. A.; Patel, D. J. *Biochemistry* **1993**, *32*, 6563.

37. Rosen, M. A.; Patel, D. J. *Biochemistry* **1993**, *32*, 6576.

38. Overmars, F. J. J.; Pikkemaat, J. A.; Van den Elst Jacques, H. H.; Boom, V.; Altona, C. *J. Mol. Biol.* **1996**, *255*, 702.

39. Pley, H. W.; Flaherty, K. M.; Mckay, D. B. *Nature (London)* **1994**, *372*, 68.

40. Scott, W. G.; Finch, J. T.; Klug, A. *Cell* **1995**, *81*, 991.

41. Tuschl, T.; Gohlke, C.; Jovin, T. M.; Westhof, E.; Eckstein, F. *Science* **1994**, *266*, 785.

42. Bassi, G. S.; Mollegaard, N. E.; Murchie, A. I. H.; Vonkitzing, E.; Lilley, D. M. J. *Nature Struct Biology* **1995**, *2*, 45.

43. Heus, H. A.; Pardi, A. *Science* **1991**, *253*, 191.

44. Seela, F.; Kaiser, K. *Nucleic Acids Res.* **1987**, *15*, 3113.

45. Komatsu, Y.; Koizumi, M. S., A.; Ohtsuka, E. *Nucleic Acids Res.* **1993**, *21*, 185.

(*Received in U.S.A.* 12 *September* 1996; *accepted* 18 *February* 1997)